Search for Dark-Matter-Induced Oscillations of Fundamental Constants Using Molecular Spectroscopy

R. Oswald, A. Nevsky, V. Vogt, and S. Schiller*
Institut für Experimentalphysik, Heinrich-Heine-Universität Düsseldorf, 40225 Düsseldorf, Germany

N. L. Figueroa, K. Zhang,† O. Tretiak, and D. Antypas‡
Johannes Gutenberg-Universität Mainz, 55128 Mainz, Germany
and Helmholtz-Institut, GSI Helmholtzzentrum für Schwerionenforschung, 55128 Mainz, Germany

D. Budker
Johannes Gutenberg-Universität Mainz, 55128 Mainz, Germany Helmholtz-Institut,
GSI Helmholtzzentrum für Schwerionenforschung, 55128 Mainz, Germany
and Department of Physics, University of California, Berkeley, California 94720, USA

A. Banerjee and G. Perez
Department of Particle Physics and Astrophysics, Weizmann Institute of Science, Rehovot, Israel 7610001

(Received 2 November 2021; revised 7 April 2022; accepted 2 June 2022; published 15 July 2022)

A possible implication of an ultralight dark matter field interacting with the standard model degrees of freedom is oscillations of fundamental constants. Here, we establish direct experimental bounds on the coupling of an oscillating ultralight dark matter field to the up, down, and strange quarks and to the gluons, for oscillation frequencies between 10 and 10^8 Hz. We employ spectroscopic experiments that take advantage of the dependence of molecular transition frequencies on the nuclear masses. Our results apply to previously unexplored frequency bands and improve on existing bounds at frequencies >5 MHz. We also improve on the bounds for coupling to the electromagnetic field and the electron field, in particular spectral windows. We identify a sector of ultralight dark matter and standard model coupling space where the bounds from equivalence principle tests may be challenged by next-generation experiments of the present kind.

DOI: 10.1103/PhysRevLett.129.031302

Introduction.—There are strong theoretical reasons to assume that fundamental constants (FC) are, in fact, dynamical and can be described as expectation values of scalar fields (see Ref. [1] for a review). Temporal evolution of these fields results in a time variation of the "constants" that can be searched for at the precision frontier (see, for example, review Ref. [2]). If a scalar field constitutes ultralight dark matter (UDM) [3,4] with sub-electron-volt mass, then its amplitude oscillates at its Compton frequency, $f_\phi = m_\phi c^2/h$, where m_ϕ is the scalar-particle mass, c is the speed of light in vacuum, and h is Planck's constant.

Two theoretical proposals relevant to this study have been put forward. In the first, the UDM mass is protected by an approximate scale-invariance symmetry [3]. In the second, UDM is an axionlike particle, whose mass is protected by an approximate shift symmetry according to the Goldstone theorem [5] that is broken, together with the combined charge-parity invariance [6,7], by two independent sectors [8]. This model is inspired by the relaxion paradigm [9]. In both frameworks, dark matter (DM) couples to the standard-model (SM) fields either due to the fact that the couplings break scale invariance [10] or via mixing with the Higgs [6], resulting in time-varying FC. An additional theoretical approach, that also leads to time-varying FC, is based on discrete symmetries [11,12].

As neither observations nor theoretical arguments can constrain the DM-particle mass [13], broadband searches are particularly motivated. Note that the preferred region of the model of Refs. [8,14] is $m_\phi \gtrsim 10^{-11}$ eV ∼ kHz, the frequency range studied here. Above roughly 10^{-18} eV, the most stringent constraints on time-varying UDM have been provided by equivalence-principle (EP) tests of gravity (see Ref. [15] and references therein). Here, we argue that there is a sense in which the bounds arising from direct DM searches are independent from any single EP test.

Using this insight we show how the EP bounds on UDM models can be challenged by atomic and molecular experiments in the near future. Prior to discussing direct searches for scalar UDM, we introduce the phenomenology of EP tests.

EP tests are conveniently expressed in terms of the Eötvös parameter, $\eta_{\rm EP}^{\rm exp} \equiv 2|\vec{a}_A - \vec{a}_B|/|\vec{a}_A + \vec{a}_B|$, that is sensitive to the differential acceleration ($\vec{a}$) of two test bodies, A and B (see Ref. [16], for example). The parameter can be expressed in terms of the relevant DM couplings to the SM fields d_i [see Eq. (1)]. One defines the "dilatonic charge" of a body, $Q_i^X = \partial \ln m_X/\partial \ln g_i$, m_X being the mass of the body X and g_i a FC. Then,

$$\eta_{\rm EP}^{\rm exp} \propto \sum_{i,j} (\Delta Q)_i^{\rm exp} d_i \times Q_j^{\rm source} d_j,$$

with the dilatonic charge difference $(\Delta Q)_i^{\rm exp} \equiv Q_i^A - Q_i^B$.

In contrast to EP-violating acceleration searches, direct scalar-UDM experiments probe observables arising from the dependence of atomic transition energies, the length of solid objects, or the refractive indices of materials on the FCs. For a review, see, for example, Ref. [17], for proposals, see Refs. [18–27], and for experiments providing bounds on FC oscillations, see Refs. [28–37]. While atomic experiments are sensitive to variation of the electron mass m_e but are almost insensitive to changes in nuclear masses m_N, molecular experiments probe for variation of both. EP tests probe nuclear masses and are largely insensitive to m_e. Thus, EP tests and oscillating FC experiments are complementary to each other, as we further discuss below.

Moreover, the level of FC oscillations might be enhanced at frequencies $f_\phi \geq 1$ kHz due to the presence of UDM halos around Earth and Sun [38] exhibiting increased DM density and coherence time. Such enhancement would not apply to fifth-force experiments, as in these, the test masses exchange virtual DM particles, a process independent of the background DM density. Recently, searches for FC oscillations were extended to frequencies $f_\phi > 1$ Hz [29,30,34,35].

While oscillations of the fine-structure constant α and m_e have received substantial attention, here, we focus on "nuclear" FCs: the quantum chromodynamics (QCD) energy scale $\Lambda_{\rm QCD} \simeq 0.33$ GeV, and the masses of the light quarks $m_{u,d,s}$. These determine m_N. Here, we employ molecular spectroscopy to search for oscillations in these FCs over a large frequency range, with a fractional sensitivity of $10^{-14} - 10^{-15}$.

Theoretical model.—To illustrate the interaction of a sub-electron-volt scalar field ϕ with SM fields, we write the low-energy effective Lagrangian as

$$\mathcal{L}_{\rm eff} \supset -\frac{\phi}{M_{\rm Pl}}\left(\sum_X d_{m_X} m_X \bar{X}X - \frac{d_\alpha}{4}F^2 + \frac{d_{g_s}\beta(g_s)}{2g_s}G^2\right). \quad (1)$$

Here, $X = e, u, d, s$ are the fermion fields with mass m_X, $F^2 = F^{\mu\nu}F_{\mu\nu}$, $G^2 = \frac{1}{2}{\rm Tr}(G^{\mu\nu}G_{\mu\nu})$, $F_{\mu\nu}$, and $G_{\mu\nu}$ are the electromagnetic field and gluon field strength, respectively, d_j are dimensionless coupling constants, and $M_{\rm Pl} = \sqrt{\hbar c/(8\pi G_N)} = 2.4 \times 10^{18}$ GeV is the Planck mass. The parameter g_s is the strong-interaction coupling constant, $\alpha_s \equiv g_s^2/4\pi$. The function $\beta(g_s)$ describes the evolution ("running") of the coupling constant with energy, via the renormalization-group equation $\beta(g_s)/(2g_s) = -(11-2n_f/3)\alpha_s/8\pi$, with n_f being the number of dynamical quarks.

As a consequence of the UDM-SM couplings in Eq. (1), the SM constants acquire a dependence on the scalar field [18],

$$m_X(\phi) = m_X\left(1 + d_{m_X}\frac{\phi}{M_{\rm Pl}}\right), \quad (2)$$

$$\alpha(\phi) \simeq \alpha\left(1 + d_\alpha \frac{\phi}{M_{\rm Pl}}\right), \quad (3)$$

$$\alpha_s(\phi) \simeq \alpha_s\left(1 - \frac{2d_{g_s}\beta(g_s)}{g_s}\frac{\phi}{M_{\rm Pl}}\right). \quad (4)$$

The QCD scale $\Lambda_{\rm QCD}$ depends on g_s through the renormalization-group equation and dimensional transmutation (see, for example, Ref. [39]). Thus, the variation of $\Lambda_{\rm QCD}$ can be written in terms of the variation of α_s as

$$\frac{\partial \ln \Lambda_{\rm QCD}}{\partial \phi} = -\frac{g_s}{2\beta(g_s)}\frac{\partial \ln \alpha_s}{\partial \phi} = \frac{d_{g_s}}{M_{\rm Pl}}. \quad (5)$$

The mass of a nucleus m_N is the sum of the nucleon masses, strong and electromagnetic binding energy. Neglecting the small electromagnetic binding energy proportional to α, the nucleon mass depends on $\Lambda_{\rm QCD}$, and $m_{u,d,s}$ [16,40]. The variation of m_N can be related to variation of FCs as [41]

$$\frac{\delta m_N}{m_N} = 0.873\frac{\Delta\Lambda_{\rm QCD}}{\Lambda_{\rm QCD}} + 0.084\frac{\Delta\hat{m}}{\hat{m}} + 3\times 10^{-4}\frac{\Delta\delta m}{\delta m} + 0.043\frac{\Delta m_s}{m_s}, \quad (6)$$

where $\hat{m} \equiv (m_u + m_d)/2$ is the mean mass of the up and down quarks and $\delta m \equiv m_u - m_d$ is the mass difference. Note that, for the contribution of m_s to the nucleon mass, we have used the lattice QCD result [41]. Combining this result with Eqs. (2) and (5), we find

$$\frac{\delta m_N}{m_N} = 0.878\hat{Q}_N \cdot \vec{d}\frac{\phi(t)}{M_{\rm Pl}}, \quad (7)$$

with $\vec{d} \equiv (d_\alpha, d_{m_e}, d_{g_s}, d_{\hat{m}}, d_{\delta m}, d_{m_s})$ and $\hat{Q}_N \approx (0, 0, 0.994, 0.096, 3\times 10^{-4}, 0.049)$ defined to be a unit-length vector.

Assuming that ϕ is a viable UDM candidate, it can be treated as a classical oscillating field,

$$\phi(\vec{x}, t) \approx m_\phi^{-1} \sqrt{2\rho_{\rm DM}^{\oplus}} \sin[m_\phi(t + \vec{\beta}_\oplus \vec{x})], \quad (8)$$

with $\rho_{\rm DM}^{\oplus}$ and $\vec{\beta}_\oplus$ being the UDM density and its typical velocity on the surface of Earth, respectively. Gravity-based measurements yield a weak direct bound on $\rho_{\rm DM}^{\oplus}$ (see, for instance, Refs. [38,42,43]).

We consider various scenarios for the properties of the DM around Earth. In the standard scenario where UDM constitutes a Galactic halo [44], with $\rho_{\rm DM}^{\oplus} \equiv \rho_{\rm DM}^{\rm G} \simeq 0.3\ {\rm GeV/cm^3}$ and $\beta_\oplus c \simeq 220$ km/s, it is reasonable to assume that during the UDM virialization process around the Galaxy, different patches or quasiparticles obtain random phases. This results in the UDM field-amplitude admitting stochastic fluctuations around its commonly assumed value [45–48]. For additional models, see Ref. [49].

Experimental approach.—Atomic clocks can be used to search for oscillations of the proton mass and the nuclear g factor. However, the operation mode of the clocks imposes $f_\phi \lesssim 1$ Hz. An alternative approach is spectroscopy of molecules [60,61]. Their transition frequencies depend on changes in the rotational and vibrational energy. Here, we focus on the latter. The vibrational energy $\hbar\omega_{\rm vib}$ of a diatomic molecule containing two nuclei N_1, N_2 scales approximately as $E_{\rm Ryd}\sqrt{m_e/\mu}$, where $\mu = m_{N_1} m_{N_2}/(m_{N_1} + m_{N_2})$ is the reduced nuclear mass. Thus, molecular transitions with a change of vibrational energy are sensitive to the nuclear mass $m_{N_i} \propto m_N$. Furthermore, their dependence on m_e is enhanced beyond the scaling $E_{\rm Ryd} \propto m_e$.

In a spectroscopy apparatus a quantum system having a resonance frequency $\nu^{(1)}$ is interrogated by the wave of frequency $\nu^{(2)}$ from an oscillator tuned to the proximity of $\nu^{(1)}$. The oscillator is often stabilized to another reference (atomic ensemble or cavity). The spectrum of the frequency deviation $\Delta\nu(t)/\nu = [\nu^{(1)}(t) - \nu^{(2)}(t)]/\nu$ is measured. The dependence of a frequency $\nu^{(i)}$ on a particular FC g may be characterized by the fractional derivative $R_g^{(i)} = d\ln\nu^{(i)}/d\ln g$. A modulation $\delta g/g$ results in a fractional frequency modulation $\delta\nu/\nu = (R_g^{(1)} - R_g^{(2)})\delta g/g$. Therefore, a key experimental parameter is the differential sensitivity $\Delta R_g = R_g^{(1)} - R_g^{(2)}$.

Apparatus and operation.—We carry out two experiments, A and B (Fig. 1) [49], in which for $\nu^{(1)}$ we use an electronic transition of molecular iodine (I_2) between the ground electronic state X and the excited electronic state B [62]. In apparatus A we perform saturation spectroscopy on the transition $R(56)32$-0 at 532 nm ($\upsilon = 0$, $\upsilon' = 32$), with sensitivity $R_N^{(1,A)} \simeq -0.06$. In apparatus B, absorption spectroscopy is implemented on the transition is $R(122)2$-10 at 725 nm ($\upsilon = 10$, $\upsilon' = 2$) [63], with $R_N^{(1,B)} \simeq 0.07$. In both experiments, the interrogating oscillator is a laser (frequency $\nu^{(2)}$). Apparatus A employs a Nd:YAG laser frequency-stabilized to a reference cavity. The detected modulation frequency range covers 10 Hz to 100 kHz. For this configuration and frequency range, $R_\alpha^{(2)} = 1$, $R_e^{(2)} = 1$ [49]. In apparatus B, the laser is a Ti:sapphire laser and frequencies in the range 100 kHz–100 MHz are considered. This range being above the acoustic cutoff frequency of the laser $f_2^{(B)} \simeq 50$ kHz [30], the frequency $\nu^{(2,B)}$ is essentially independent of the FCs [64].

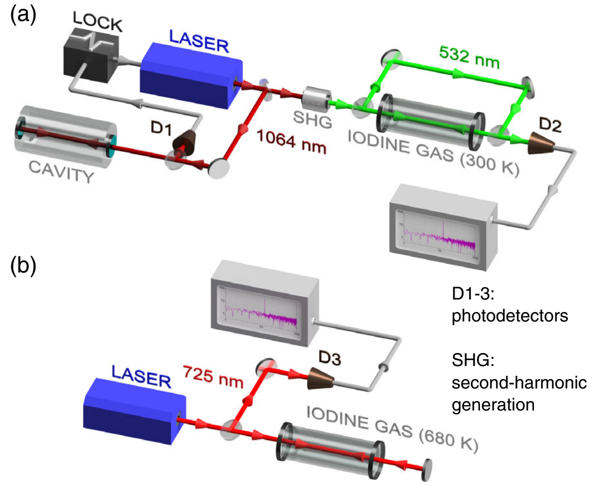

FIG. 1. The two molecular iodine experiments: (a) A; (b) B.

Summarizing, experiments A and B provide sensitivity to α, m_e, and m_N. For experiment A, $\Delta R_\alpha^{(A)} \simeq 2-1 = 1$, $\Delta R_e^{(A)} = (1 - R_N^{(1,A)}) - 1 \simeq +0.06$, $\Delta R_N^{(A)} = R_N^{(1,A)} - 0 \simeq -0.06$. For experiment B, $\Delta R_\alpha^{(B)} \simeq 2$, $\Delta R_e^{(B)} = (1 - R_N^{(1,B)}) - 0 \simeq +0.93$, and $\Delta R_N^{(B)} = R_N^{(1,B)} - 0 \simeq 0.07$.

In both experiments, the instantaneous frequency deviation $\Delta\nu$ is converted into a voltage signal $V^{(k)}(t) = D^{(k)}\Delta\nu^{(k)}(t)$, with the discriminators $D^{(k)}$ being system parameters, and $k = A, B$. This allows obtaining the spectrum of the fractional frequency variation $\delta\nu^{(k)}/\nu^{(k)}$. The time-varying FC ($\alpha$, m_e, and m_N) contribute to the variation according to

$$\frac{\delta\nu^{(k)}}{\nu^{(k)}} = \Delta R_\alpha^{(k)}\frac{\delta\alpha}{\alpha} + \Delta R_e^{(k)}\frac{\delta m_e}{m_e} + \Delta R_N^{(k)}\frac{\delta m_N}{m_N}. \quad (9)$$

Search for oscillating fundamental constants.—In the experiments, the lasers are tuned to the iodine transitions and the signals $V^{(k)}(t)$ are recorded. From these records the periodograms are calculated [49]. In experiment A, the obvious peaks in the periodogram [49] were investigated and identified as being of technical origin, in part by shifting the laser frequency away from the resonance and repeating the measurement. This left no obvious candidate UDM signals. We do not give limits for these excluded intervals, that have widths of 5 Hz or smaller. From the

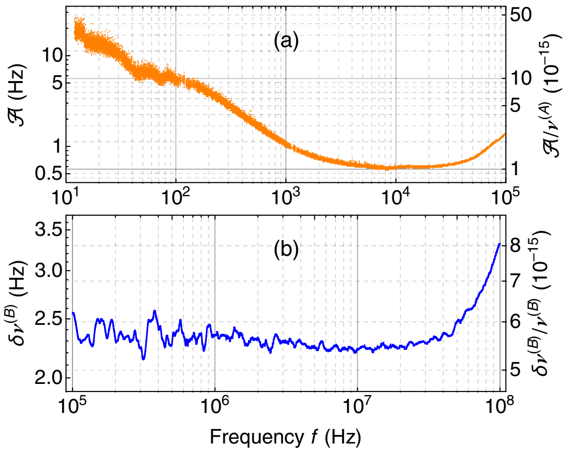

FIG. 2. (a) Experiment A. Spectral amplitude $\mathcal{A} = \sqrt{\mathrm{PSD}_F/T}$ of the scaled discriminator signal $\Delta\nu^{(A)}(t) = V^{(A)}(t)/D^{(A)}$. PSD_F is the optimally filtered power spectral density, with a filter adapted to signals having the same linewidth f/Q_0, $Q_0 \simeq 1\times 10^6$, as standard Galactic halo UDM. The width of the orange band corresponds to the mean of $\mathcal{A} \pm \sigma(f)$. (b) Experiment B. The bound (95% confidence level) on fluctuations of the signal $\Delta\nu^{(B)}(t) = V^{(B)}(t)/D^{(B)}$.

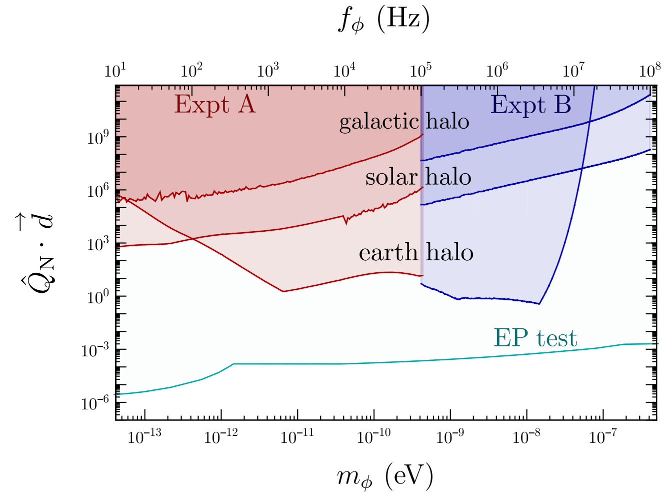

FIG. 3. Exclusion plot of the combination of couplings to the QCD sector, $\hat{Q}_N \cdot \vec{d} = 0.994 d_{g_s} + 0.096 d_{\hat{m}} + 3\times 10^{-4} d_{\delta m} + 0.049 d_{m_s}$. Turquoise line: fifth-force–EP-violation experiments [66–70].

periodogram, the upper limit of the coupling parameters d_g was determined using the analysis of Ref. [52]. The (model-dependent) spectral amplitude of the recorded signal is shown in Fig. 2(a) [49].

In experiment B, the voltage $V(t)$ was measured with the laser frequency tuned either on the slope of the I_2 resonance, or off resonance, alternating between these UDM-sensitive and insensitive acquisition modes to account for spurious signals due to sources other than UDM. The corresponding periodograms were computed and continuously averaged. The periodogram difference between the on- and off-resonance acquisition modes was also computed and averaged over a 60-hr-long run. This spectrum will contain power in excess of statistical noise in the presence of FC oscillations, and it is subsequently investigated for UDM detection. A number of candidate peaks were identified having power in excess of a 95% detection threshold, that was computed considering the "look elsewhere" effect [65]. All spurious signals were checked in auxiliary experiments and eventually attributed to technical noise. The postinspected spectrum is used to obtain a constraint for $\delta\nu^{(B)}/\nu^{(B)}$ Fig. 2(b) [49].

Models and bounds.—We analyze the experimental data within the three mentioned models that differ in terms of the UDM field amplitude and its coherence time $\tau_{\mathrm{coh}} = 1/[\omega_\phi (v_{\mathrm{vir}}/c)^2]$:

$$\tau_{\mathrm{coh}} = \begin{cases} 5.9\times 10^5 f_\phi^{-1}, Q = 1.1\times 10^6, & \text{Galactic halo} \\ 7.1\times 10^7 f_\phi^{-1}, Q = 9.0\times 10^7, & \text{Solar halo} \\ \infty, & \text{Earth halo.} \end{cases} \quad (10)$$

To derive bounds to the UDM couplings, we assume that only one of the constants m_e, α, or m_N in Eq. (9) oscillates and analyze the three cases separately [49]. In Fig. 3, we present our constraints on the combined quark and gluons couplings $\hat{Q}_N \cdot \vec{d}$ together with existing EP constraints.

Constraints on the variation of α and m_e are presented in Fig. 4, alongside the strongest previous constraints on the relevant parameter space. Astrophysical bounds on our scenario could also apply, however, these are typically weaker than those discussed here and are less robust (see Refs. [71–73] for recent discussions). For clarity, we show constraints for the standard Galactic UDM halo only. Our results cover the previously unexplored bands 10–50 Hz and 5–10 kHz, and improve on existing bounds in the ranges 0.1–0.2 MHz and 3–100 MHz.

More generally, our experiments are sensitive to the following linear combinations of the full set of couplings, defined in Eqs. (7), (9), that can be written as $\vec{Q}\cdot\vec{d} = |\vec{Q}|\hat{Q}\cdot\vec{d}$ with $|\vec{Q}^A| = 1$, $|\vec{Q}^B| = 2.21$, and the unit-length vectors

$$\hat{Q}^A \simeq (1.0, 0.06, -0.05, -0.005, -1.5\times 10^{-5}, -0.0024),$$
$$\hat{Q}^B \simeq (0.90, 0.42, 0.027, 0.0025, 8\times 10^{-6}, 0.0013). \quad (11)$$

We do not consider the strange quark mass contribution in the context of EP as it is complementary to the contribution of g_s, see Ref. [49]. Thus, for the following discussion of the complementarity between EP tests and UDM searches, we reduce the six-dimensional $\vec{Q}$ to five dimensions by dropping the last entry corresponding to m_s. In this space, one can find a direction $\hat{Q}^{\perp}_{\mathrm{full}}(m_\phi)$ that is

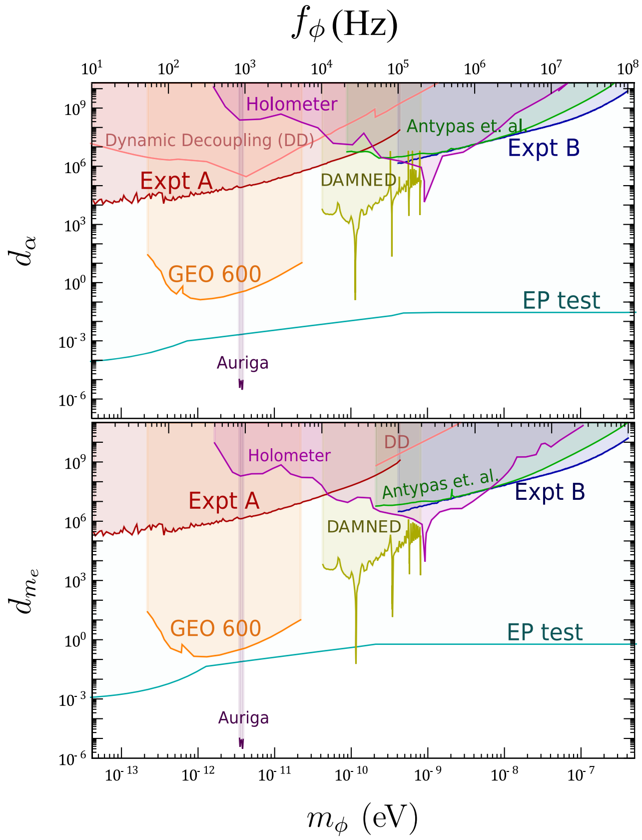

FIG. 4. Exclusion plot of the UDM couplings to α (top) and m_e (bottom). Existing constraints: shaded regions in orange [34], yellow [35], pink [29], green [64], magenta [37], and purple [74]. Fifth-force–EP tests: turquoise [66–70].

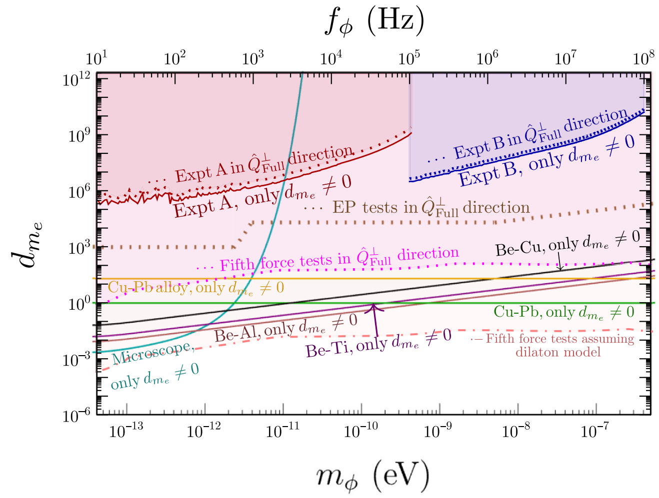

FIG. 5. Exclusion plot for d_{m_e}. The dotted lines depict the bounds for a model defined by a vector of sensitivities, $\hat{Q}^\perp_{\rm full}(m_\phi)$, that is orthogonal to the sensitivities of four leading EP test experiments [49]. Bounds from other published experiments, shown in Fig. 4, are not shown again here. The bound from the fifth-best EP test experiment in a given mass range, projected onto the $\hat{Q}^\perp_{\rm full}(m_\phi)$ direction, and further on the d_{m_e} direction, is shown as dotted brown line.

orthogonal to the best four EP-test bounds, for a given mass. For example, in the mass range of $2\times 10^{-12} \lesssim m_\phi/\mathrm{eV} \lesssim 5\times 10^{-9}$, these are the Be-Al [66], Be-Ti [67], Cu-Pb [75], and Be-Cu [76] experiments, and we find $\hat{Q}^\perp_{\rm full}(m_\phi) \simeq (0.003, 0.987, 0.002, -0.001, 0.160)$. For masses above 5×10^{-9} eV, $\hat{Q}^\perp_{\rm full}$ is perpendicular to the Be-Al [66], Be-Ti [67], Cu-Pb [75], and Cu-Pb-alloy [77] sensitivity vectors, with a correspondingly modified $\hat{Q}^\perp_{\rm full}$ [49]. Models of light scalar UDM with coupling direction defined according to $\hat{Q}^\perp_{\rm full}(m_\phi)\cdot\vec{d}$ would not be constrained by these four leading EP bounds. Note that, $\hat{Q}^\perp_{\rm full}(m_\phi)$ has a substantial overlap with the d_{m_e} direction (the second entry) throughout the whole mass range. Thus, experiments that are particularly sensitive to m_e, test a sector of coupling space that the first four-best EP experiments are weakly sensitive to. In Fig. 5, we present our bounds on $\hat{Q}^\perp_{\rm full}\cdot\vec{d}$, projected (for clarity) in the d_{m_e} direction as dotted red and blue lines. The fifth-best EP bound projected onto $\hat{Q}^\perp_{\rm full}(m_\phi)$ and further on d_{m_e}, is shown by a brown dotted line. Note that we could only calculate the projection of $\hat{Q}^\perp_{\rm full}$ into the remaining fifth-best EP bound to an accuracy of 1 part in 10^3 due to the limited precision of the published test mass composition data. We find that in this sector of coupling space the bounds related to our direct UDM experiments are only two to 3 orders weaker than those from EP tests.

Furthermore, one can consider a model of a dilaton UDM, which is not constrained by the EP violating tests [18] (see Ref. [49]). A dilaton UDM would mediate a long-range Yukawa force, which can be constrained by various experiments that test for deviations from Newtonian gravity (fifth-force searches) [78]. The fifth-force bound for this model is represented by the crimson colored dot-dashed line, while for completeness in pink we also show the fifth-force bound for our model where the coupling is defined according to $\hat{Q}^\perp_{\rm full}(m_\phi)\cdot\vec{d}$ as discussed above.

Conclusion.—Our molecular-spectroscopy experiments have resulted in the first bounds on the coupling of an oscillating UDM field to the gluon and quark fields, in a broad frequency range that spans seven decades (10 Hz–100 MHz). In four windows within this range, improvements on previous limits for the coupling to the electromagnetic field and the electron field were also obtained.

A new generation of experiments, with minimization of all noise sources, long acquisition times, high sampling rates, and, possibly, multiple setups to improve statistical averaging, could improve the present limits by several orders of magnitude. Furthermore, we have argued that there is a special class of dark matter couplings where the bounds from equivalence principle tests are significantly less stringent than expected. Consequently, future experiments of the present kind may be able to probe this class of UDM models with sensitivity competitive to EP tests.

We thank D. Kanta for help with the project, and D. Iwaschko and R. Gusek for electronics development. A. B. thanks the Galileo Galilei Institute for Theoretical Physics for the hospitality and the INFN for partial support during the completion of this work. This work was supported by the Cluster of Excellence "Precision Physics, Fundamental Interactions, and Structure of Matter" (PRISMA + EXC 2118/1) funded by the German Research Foundation (DFG) within the German Excellence Strategy (Project ID 39083149), by the European Research Council (ERC) under the European Union Horizon 2020 research and innovation program (project Dark-OST, Grant No. 695405, project YbFUN, Grant No. 947696), by the DFG Reinhart Koselleck project. The work of A. B. was supported by the Azrieli Foundation. The work of G. P. is supported by grants from BSF-NSF (No. 2019760), Friedrich Wilhelm Bessel research award, GIF, the ISF (Grant No. 718/18), Minerva, SABRA–Yeda-Sela–WRC Program, the Estate of Emile Mimran, and The Maurice and Vivienne Wohl Endowment.

[*]step.schiller@hhu.de
[†]kezhang@uni-mainz.de
[‡]dantypas@uni-mainz.de

[1] J.-P. Uzan, Living Rev. Relativity **14**, 2 (2011).
[2] M. S. Safronova, D. Budker, D. DeMille, D. F. J. Kimball, A. Derevianko, and C. W. Clark, Rev. Mod. Phys. **90**, 025008 (2018).
[3] A. Arvanitaki, J. Huang, and K. Van Tilburg, Phys. Rev. D **91**, 015015 (2015).
[4] P. W. Graham, D. E. Kaplan, J. Mardon, S. Rajendran, and W. A. Terrano, Phys. Rev. D **93**, 075029 (2016).
[5] F. Chadha-Day, J. Ellis, and D. J. E. Marsh, Sci. Adv. **8**, eabj3618 (2022).
[6] T. Flacke, C. Frugiuele, E. Fuchs, R. S. Gupta, and G. Perez, J. High Energy Phys. 06 (2017) 050.
[7] K. Choi and S. H. Im, J. High Energy Phys. 12 (2016) 093.
[8] A. Banerjee, H. Kim, and G. Perez, Phys. Rev. D **100**, 115026 (2019).
[9] P. W. Graham, D. E. Kaplan, and S. Rajendran, Phys. Rev. Lett. **115**, 221801 (2015).
[10] W. D. Goldberger, B. Grinstein, and W. Skiba, Phys. Rev. Lett. **100**, 111802 (2008).
[11] A. Hook, Phys. Rev. Lett. **120**, 261802 (2018).
[12] D. Brzeminski, Z. Chacko, A. Dev, and A. Hook, Phys. Rev. D **104**, 075019 (2021).
[13] G. Bertone and T. M. P. Tait, Nature (London) **562**, 51 (2018).
[14] A. Banerjee, E. Madge, G. Perez, W. Ratzinger, and P. Schwaller, Phys. Rev. D **104**, 055026 (2021).
[15] G. M. Tino, L. Cacciapuoti, S. Capozziello, G. Lambiase, and F. Sorrentino, Prog. Part. Nucl. Phys. **112**, 103772 (2020).
[16] T. Damour and J. F. Donoghue, Phys. Rev. D **82**, 084033 (2010).
[17] M. S. Safronova, Ann. Phys. (Amsterdam) **531**, 1800364 (2019).
[18] A. Arvanitaki, J. Huang, and K. Van Tilburg, Phys. Rev. D **91**, 015015 (2015).
[19] M. S. Safronova, S. G. Porsev, C. Sanner, and J. Ye, Phys. Rev. Lett. **120**, 173001 (2018).
[20] V. A. Dzuba, V. V. Flambaum, and S. Schiller, Phys. Rev. A **98**, 022501 (2018).
[21] A. Banerjee, H. Kim, O. Matsedonskyi, G. Perez, and M. S. Safronova, J. High Energy Phys. 07 (2020) 153.
[22] E. Peik, T. Schumm, M. S. Safronova, A. Pálffy, J. Weitenberg, and P. G. Thirolf, Quantum Sci. Technol. **6**, 034002 (2021).
[23] J. Manley, D. J. Wilson, R. Stump, D. Grin, and S. Singh, Phys. Rev. Lett. **124**, 151301 (2020).
[24] A. A. Geraci, C. Bradley, D. Gao, J. Weinstein, and A. Derevianko, Phys. Rev. Lett. **123**, 031304 (2019).
[25] Y. V. Stadnik and V. V. Flambaum, Phys. Rev. Lett. **114**, 161301 (2015).
[26] Y. V. Stadnik and V. V. Flambaum, Phys. Rev. A **93**, 063630 (2016).
[27] H. Grote and Y. V. Stadnik, Phys. Rev. Research **1**, 033187 (2019).
[28] K. Van Tilburg, N. Leefer, L. Bougas, and D. Budker, Phys. Rev. Lett. **115**, 011802 (2015).
[29] S. Aharony, N. Akerman, R. Ozeri, G. Perez, I. Savoray, and R. Shaniv, Phys. Rev. D **103**, 075017 (2021).
[30] D. Antypas, O. Tretiak, A. Garcon, R. Ozeri, G. Perez, and D. Budker, Phys. Rev. Lett. **123**, 141102 (2019).
[31] A. Hees, J. Guéna, M. Abgrall, S. Bize, and P. Wolf, Phys. Rev. Lett. **117**, 061301 (2016).
[32] C. J. Kennedy, E. Oelker, J. M. Robinson, T. Bothwell, D. Kedar, W. R. Milner, G. E. Marti, A. Derevianko, and J. Ye, Phys. Rev. Lett. **125**, 201302 (2020).
[33] P. Wcislo *et al.*, Sci. Adv. **4**, eaau4869 (2018).
[34] S. M. Vermeulen *et al.*, Nature (London) **600**, 424 (2021).
[35] E. Savalle, A. Hees, F. Frank, E. Cantin, P.-E. Pottie, B. M. Roberts, L. Cros, B. T. McAllister, and P. Wolf, Phys. Rev. Lett. **126**, 051301 (2021).
[36] W. M. Campbell, B. T. McAllister, M. Goryachev, E. N. Ivanov, and M. E. Tobar, Phys. Rev. Lett. **126**, 071301 (2021).
[37] L. Aiello, J. W. Richardson, S. M. Vermeulen, H. Grote, C. Hogan, O. Kwon, and C. Stoughton, Phys. Rev. Lett. **128**, 121101 (2022).
[38] A. Banerjee, D. Budker, J. Eby, H. Kim, and G. Perez, Commun. Phys. **3**, 1 (2020).
[39] M. E. Peskin and D. V. Schroeder, *An Introduction to Quantum Field Theory* (Addison-Wesley, Reading, USA, 1995).
[40] M. A. Shifman, A. I. Vainshtein, and V. I. Zakharov, Phys. Lett. **78B**, 443 (1978).
[41] P. M. Junnarkar and A. Walker-Loud, Phys. Rev. D **87**, 114510 (2013).
[42] C. J. Hogan and M. J. Rees, Phys. Lett. B **205**, 228 (1988).
[43] N. B. Anderson, A. Partenheimer, and T. D. Wiser, arXiv: 2007.11016.
[44] D. J. E. Marsh, Phys. Rep. **643**, 1 (2016).

[45] J. W. Foster, N. L. Rodd, and B. R. Safdi, Phys. Rev. D **97**, 123006 (2018).

[46] G. P. Centers, J. W. Blanchard, J. Conrad, N. L. Figueroa, A. Garcon, A. V. Gramolin, D. F. J. Kimball, M. Lawson, B. Pelssers, J. A. Smiga *et al.*, Nat. Commun. **12**, 7321 (2021).

[47] M. Lisanti, M. Moschella, and W. Terrano, Phys. Rev. D **104**, 055037 (2021).

[48] A. V. Gramolin, A. Wickenbrock, D. Aybas, H. Bekker, D. Budker, G. P. Centers, N. L. Figueroa, D. F. Jackson Kimball, and A. O. Sushkov, Phys. Rev. D **105**, 035029 (2022).

[49] See Supplemental Material at http://link.aps.org/supplemental/10.1103/PhysRevLett.129.031302 for details on the experimental setups, data evaluation, and the discussion of additional models and EP tests, which includes Refs. [50–59].

[50] J. P. Turneaure, C. M. Will, B. F. Farrell, E. M. Mattison, and R. F. C. Vessot, Phys. Rev. D **27**, 1705 (1983).

[51] E. Savalle, A. Hees, F. Frank, E. Cantin, P.-E. Pottie, B. M. Roberts, L. Cros, B. T. McAllister, and P. Wolf, Phys. Rev. Lett. **126**, 051301 (2021).

[52] A. Derevianko, Phys. Rev. A **97**, 042506 (2018).

[53] A. Derevianko (private communication).

[54] M. S. Turner, Phys. Rev. D **42**, 3572 (1990).

[55] P. Touboul, G. Metris, M. Rodrigues, Y. Andre, Q. Baghi *et al.*, Phys. Rev. Lett. **119**, 231101 (2017).

[56] A. Dymarsky, Z. Komargodski, A. Schwimmer, and S. Theisen, J. High Energy Phys. 10 (2015) 171.

[57] F. Coradeschi, P. Lodone, D. Pappadopulo, R. Rattazzi, and L. Vitale, J. High Energy Phys. 11 (2013) 057.

[58] T. R. Taylor and G. Veneziano, Phys. Lett. B **213**, 450 (1988).

[59] D. B. Kaplan and M. B. Wise, J. High Energy Phys. 08 (2000) 037.

[60] D. Hanneke, B. Kuzhan, and A. Lunstad, Quantum Sci. Technol. **6**, 014005 (2021).

[61] D. Antypas, O. Tretiak, K. Zhang, A. Garcon, G. Perez, M. G. Kozlov, S. Schiller, and D. Budker, Quantum Sci. Technol. **6**, 034001 (2021).

[62] S. Gerstenkorn and P. Luc, J. Phys. France **46**, 867 (1985).

[63] S. Rakowsky, D. Zimmermann, and W. E. Ernst, Appl. Phys. B **48**, 463 (1989).

[64] D. Antypas, D. Budker, V. V. Flambaum, M. G. Kozlov, G. Perez, and J. Ye, Ann. Phys. (Amsterdam) **532**, 1900566 (2020).

[65] J. D. Scargle, Astrophys. J. **263**, 835 (1982).

[66] T. A. Wagner, S. Schlamminger, J. H. Gundlach, and E. G. Adelberger, Classical Quantum Gravity **29**, 184002 (2012).

[67] S. Schlamminger, K. Y. Choi, T. A. Wagner, J. H. Gundlach, and E. G. Adelberger, Phys. Rev. Lett. **100**, 041101 (2008).

[68] G. L. Smith, C. D. Hoyle, J. H. Gundlach, E. G. Adelberger, B. R. Heckel, and H. E. Swanson, Phys. Rev. D **61**, 022001 (1999).

[69] J. Bergé, P. Brax, G. Métris, M. Pernot-Borràs, P. Touboul, and J.-P. Uzan, Phys. Rev. Lett. **120**, 141101 (2018).

[70] A. Hees, O. Minazzoli, E. Savalle, Y. V. Stadnik, and P. Wolf, Phys. Rev. D **98**, 064051 (2018).

[71] R. Budnik, H. Kim, O. Matsedonskyi, G. Perez, and Y. Soreq, Phys. Rev. D **104**, 015012 (2021).

[72] W. DeRocco, P. W. Graham, and S. Rajendran, Phys. Rev. D **102**, 075015 (2020).

[73] N. Bar, K. Blum, and G. D'Amico, Phys. Rev. D **101**, 123025 (2020).

[74] A. Branca, M. Bonaldi, M. Cerdonio, L. Conti, P. Falferi, F. Marin, R. Mezzena, A. Ortolan, G. A. Prodi, L. Taffarello, G. Vedovato, A. Vinante, S. Vitale, and J.-P. Zendri, Phys. Rev. Lett. **118**, 021302 (2017).

[75] G. L. Smith, C. D. Hoyle, J. H. Gundlach, E. G. Adelberger, B. R. Heckel, and H. E. Swanson, Phys. Rev. D **61**, 022001 (1999).

[76] Y. Su, B. R. Heckel, E. G. Adelberger, J. H. Gundlach, M. Harris, G. L. Smith, and H. E. Swanson, Phys. Rev. D **50**, 3614 (1994).

[77] P. G. Nelson, D. M. Graham, and R. D. Newman, Phys. Rev. D **42**, 963 (1990).

[78] E. Fischbach and C. Talmadge, in *Proceedings of the 31st Rencontres de Moriond: Dark Matter and Cosmology, Quantum Measurements and Experimental Gravitation* (1996), pp. 443–451, arXiv:hep-ph/9606249.